LETTERS

Social diversity promotes the emergence of cooperation in public goods games

Francisco C. Santos[1], Marta D. Santos[2] & Jorge M. Pacheco[2]

Humans often cooperate in public goods games[1–3] and situations ranging from family issues to global warming[4,5]. However, evolutionary game theory predicts[4,6] that the temptation to forgo the public good mostly wins over collective cooperative action, and this is often also seen in economic experiments[7]. Here we show how social diversity provides an escape from this apparent paradox. Up to now, individuals have been treated as equivalent in all respects[4,8], in sharp contrast with real-life situations, where diversity is ubiquitous. We introduce social diversity by means of heterogeneous graphs and show that cooperation is promoted by the diversity associated with the number and size of the public goods game in which each individual participates and with the individual contribution to each such game. When social ties follow a scale-free distribution[9], cooperation is enhanced whenever all individuals are expected to contribute a fixed amount irrespective of the plethora of public goods games in which they engage. Our results may help to explain the emergence of cooperation in the absence of mechanisms based on individual reputation and punishment[10–12]. Combining social diversity with reputation and punishment will provide instrumental clues on the self-organization of social communities and their economical implications.

The *N*-person prisoner's dilemma constitutes the most used metaphor to study public goods games (PGGs): cooperators (C) contribute an amount c ('cost') to the public good; defectors (D) do not contribute. The total contribution is multiplied by an enhancement factor r and the result is equally distributed between all N members of the group. Hence, Ds get the same benefit of the Cs at no cost. Collective action to shelter, protect and nourish, which abounds in the animal world, provides examples of PGGs, because the cooperation of group members is required. Ultimately, the success (and survival)[5] of the human species relies on the capacity of humans for large-scale cooperation. In the absence of enforcement mechanisms[7,13,14], conventional evolutionary game theory predicts that the temptation to defect leads individuals to forgo the public good[4] in the *N*-person prisoner's dilemma. Whenever interactions are not repeated, and reward and punishment[4,8,13] can be ruled out, several mechanisms were explored that promote cooperation. Individuals were either constrained to interact only with their neighbours on spatial lattices[4,8,15], or given the freedom to opt out of participating[4,15], leading to a coexistence of cooperators and defectors, even on spatial lattices.

Here we investigate what happens in the absence of reputation and punishment and when participation is compulsory. Unlike previous studies involving PGGs[4,8,15], individuals now interact along the social ties defined by a heterogeneous graph[16–18]. This reflects the fact that individuals have different roles in social communities. Empirical studies show that social graphs have a marked degree of heterogeneity combined with small-world effects[19–21], as illustrated in Fig. 1b. Hence we introduce diversity in the study of cooperation under PGGs in the context of evolutionary graph theory[22], and in the presence of spatial and network reciprocity[18,23,24].

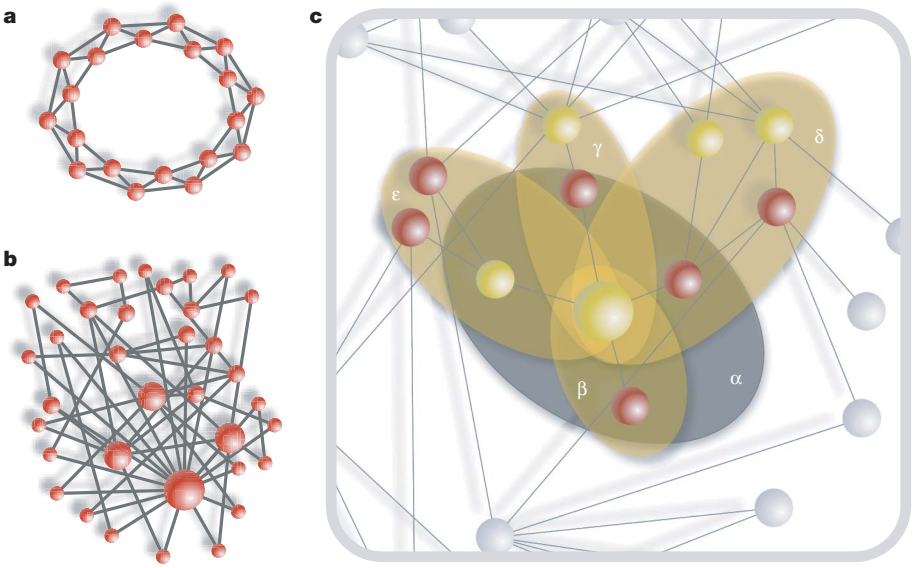

Figure 1 | Population structure and local neighbourhoods. a, Regular graphs studied so far, which mimic spatially extended systems. **b**, Scale-free graphs[9] in which small-world effects coexist with a large heterogeneity in neighbourhood size. **c**, The focal individual (largest sphere) belongs to different groups (neighbourhoods) of different sizes in a heterogeneous graph. Given his/her connectivity $k = 4$, we identify five neighbourhoods, each centred on one of the members of the focal individual's group, such that individual fitness derives from the payoff accumulated in all five neighbourhoods (α, β, γ, δ and ε).

[1]Institut de Recherches Interdisciplinaires et de Développements en Intelligence Artificielle (IRIDIA), Computer and Decision Engineering Department, Université Libre de Bruxelles, B-1050 Brussels, Belgium. [2]ATP-group, Centro de Física Teórica e Computacional (CFTC) and Departamento de Física da Universidade de Lisboa, Complexo Interdisciplinar, Av. Prof. Gama Pinto 2, 1649-003 Lisboa, Portugal.

Figure 1c shows how diversity is introduced, in which we enumerate the different PGGs in which the focal individual (large sphere) engages. Each PGG is associated with a fixed neighbourhood defined by the social graph; given the focal individual's connectivity $k = 4$, he/she participates in five PGGs; that centred in his/her neighbourhood α (group size of 5) plus those associated with the neighbourhoods centred on his/her neighbours: β (2), γ (3), δ (5) and ε (4). Hence graph heterogeneity leads individuals to engage in different numbers of PGGs with different group sizes. Furthermore, there is no reason for every C to contribute the same amount to each game in which he/she participates (see below).

Figure 2a shows results for the evolution of cooperation corresponding to the conventional situation in which every C pays a fixed cost c in every game that he/she plays. We plot the fraction of cooperators in the population that survive evolution as a function of the renormalized PGG enhancement factor $\eta = r/(z+1)$, where z is the average connectivity of the population graph (see Methods). In infinite, well-mixed populations, a sharp transition from defection to cooperation takes place at $\eta = 1$. Comparison between the results obtained on regular graphs (Fig. 1a) with those on strongly heterogeneous graphs (scale-free; Fig. 1b) reveal the sizable impact of heterogeneity on the evolution of cooperation. For regular graphs (in which, from the perspective of a population structure, every individual is equivalent to any other) cooperators become predominant (their fraction exceeds 50%) at $\eta \approx 0.7$: network reciprocity[18,23,24] leads to an enhancement of cooperation also under PGGs[4,8,15]. This number decreases to $\eta \approx 0.6$ on scale-free graphs, in which individual participation now reflects both a diversity in the size of each individual's PGGs and in the different number of PGGs in which each individual participates.

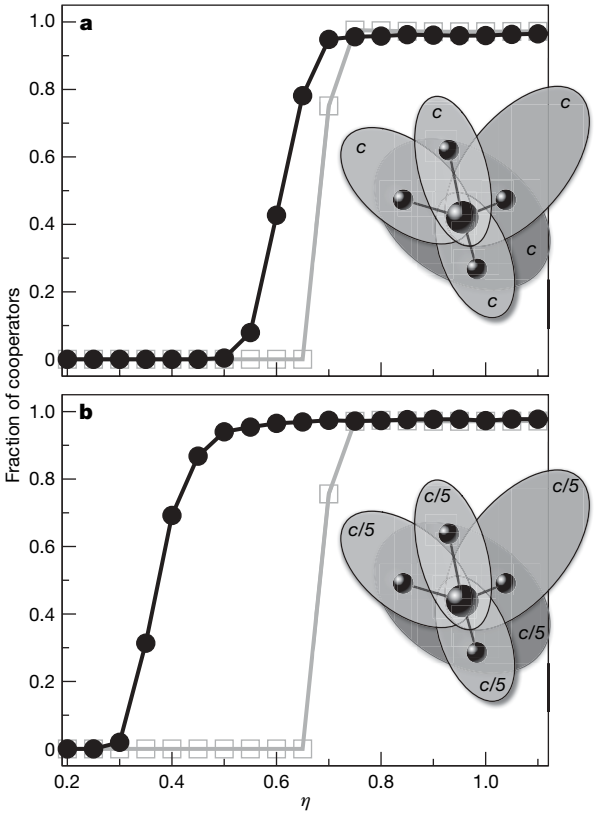

Figure 2 | Evolution of cooperation in networked PGGs. Black lines and filled circles show results for scale-free graphs; grey lines and open squares show results for regular graphs. In all cases $z = 4$. **a**, Fixed cost per game. Cs pay a cost $c = 1$ for each PGG in which they participate: diversity in number of PGGs and size of each PGG associated with scale-free graphs merits a significant enhancement of cooperation. **b**, Fixed cost per individual. Each C contributes a total cost c equally shared between all $k + 1$ PGGs in which he/she engages. This change of model leads to an impressive boost of cooperation.

The contribution of each C in Fig. 2a has been proportional to $k + 1$, where k is the number of neighbours (vertex degree). This may be unrealistic, because individuals have limited resources and social rules often accommodate a more egalitarian overall contribution from individuals[25]. In the extreme opposite limit, all Cs contribute the same overall cost, equally shared between all games in which each individual participates. In this limit, still another new type of diversity is introduced—that of individual contributions to each game. Real-world situations will naturally fall somewhere between these limits, as individuals learn[26] to cooperate (or defect) in better ways. In general, however, one expects diversity of contributions from individuals. Depending on the problem at stake, any contribution may be necessary and even welcome, however small. Below we show that, whenever all contributions are interpreted as acts of cooperation, cooperation blooms.

Figure 2b shows the results including this additional diversity in which Cs contribute $c/(k+1)$ for each game, k being their degree in the social graph. This new model leads to an impressive boost of cooperation. In all cases, cooperation now dominates for values of η below 0.4.

What is the origin of such a boost of cooperation? Because each C now contributes $c/(k+1)$ to each game, diversity resulting from heterogeneous graphs determines a richer spectrum of individual fitness. In a single PGG, the fitness difference between a C and a D is no longer constant and proportional to c, as on homogeneous graphs, but now depends on the social context of the individual. As shown in detail in Supplementary Information, the highly connected nodes (hubs) are those that turn most quickly into cooperation. This is because, under this contribution model, the relative fitness of a single cooperator increases with its connectivity, as illustrated in Fig. 3 (derivation details are given in Supplementary Information). Consequently, heterogeneity confers a natural advantage on hubs. In practice, Cs survive extinction for values of η about 0.25. Because $z = 4$, $\eta = 0.25$ implies that $r = 1.25$, much lower than the size $N = 3$ of the smallest group in the entire population. Note that, in those games for which $\eta_k \equiv r/(k+1) > 1$ (the smaller groups), the social dilemma might become relaxed, because in this case it is better to play C than D. As Fig. 2b shows, cooperation prevails despite $\eta_k < 1$ in every PGG played. In fact, the impact of diversity is preserved even when the social dilemma is transformed such that defection is always preferred, irrespective of η.

It still remains to explain how a D sitting on a large hub can be taken over by a C. As shown in the Supplementary Information, Ds are victims of their own success—successful Ds breed Ds in their neighbourhood, inducing a negative feedback mechanism that reduces their fitness[27]. Consequently, they become vulnerable to nearby cooperators. Once invaded by a C, a hub will remain C, as by placing Cs on nearby sites, successful Cs increase their fitness. The role of Cs is therefore crucial and twofold: they efficiently disseminate the cooperator strategy across social networks, whereas they get a stronghold on hubs by minimizing the potential loss from exploitation by free-riding Ds. It is noteworthy that the results shown in Fig. 2b, in which selection is strong, are robust with respect to the detailed evolutionary dynamics (pairwise comparison[28], birth–death[18], death–birth[18]), to the updating strategy (synchronous, asynchronous), and even to errors (mutations cannot destroy C-dominance).

What about the defectors? They have a minor role as social parasites when they survive on such graphs. Figure 2b shows that some residual Ds continue to exploit Cs. In the Supplementary Information we provide a detailed analysis showing how the evolutionary dynamics inexorably leads cooperators to invade the hubs quickly, whereas defectors are able to survive only on loosely connected nodes, with low fitness and exploiting cooperators of low fitness.

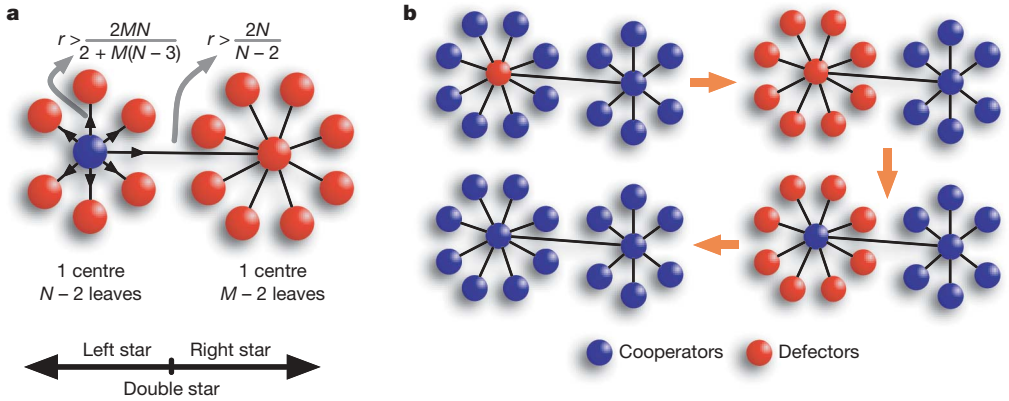

Figure 3 | Dynamics on the double star. a, When a single C (blue) occupies the centre of the left star, the critical r above which his/her fitness exceeds that of any of the leaves decreases whenever the size (number of leaves) of the left star increases or the size of the right star decreases. Taking over the D (red) on the right centre does not depend on his/her connectivity. **b**, When a D occupies a high-fitness location, the fact that he/she places other Ds in his/her neighbourhood leads to his/her own demise (see Supplementary Information for details).

In a more economical perspective, our results also portray different evolutionary outcomes even in communities in which all individuals cooperate. Now we consider populations of 100% cooperators and look at their 'wealth' (fitness) distribution according to different underlying models. We consider homogeneous (regular) and heterogeneous (scale-free) graphs. In Fig. 4 we plot the fraction of the population that holds a given fraction of the total wealth.

The differences are striking. On regular graphs an egalitarian wealth distribution is obtained, irrespective of the contribution model. On scale-free graphs wealth distributions follow a power law. However, for a fixed cost per individual, the population has significantly fewer poor and more rich (note the logarithmic scale in Fig. 4). Given that the emergence of cooperation is easiest in this case, the results provide an impressive account of the role of diversity and its implications in both the emergence of cooperation and the resulting wealth distribution.

In this study any contribution has been identified with cooperation. In communities under the influence of social norms, individual contributions will be easily classified as acts of cooperation (or not). In this context, our results suggest the possibility that successful communities are those in which the act of giving is more important than the amount given. This may be of particular relevance whenever the survival of the community is at stake, in which case any help is necessary[14,25]. Most probably, in such cases selection is strong, as considered here.

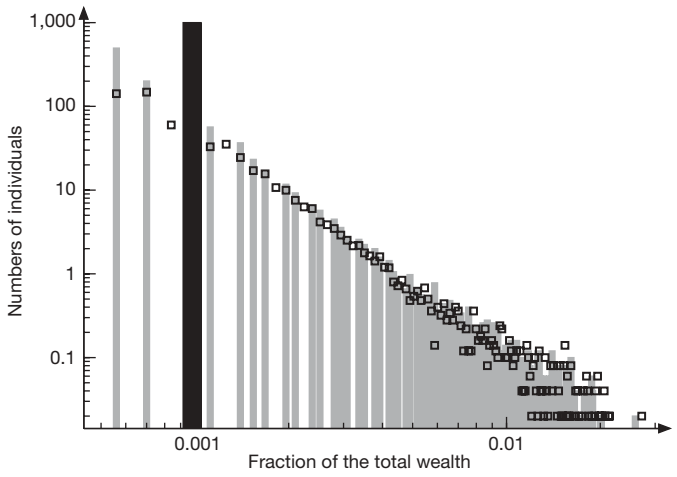

Figure 4 | Wealth distribution. On scale-free graphs, the wealth (fitness) distribution follows a power law, both when each individual invests a fixed cost per game (thin grey bars) or when he/she spends an overall fixed cost (open squares). The latter case leads to communities with fewer 'poor' and more 'rich'. These behaviours contrast with the egalitarian wealth distribution characteristic of homogeneous graphs (thick black bar).

METHODS SUMMARY

According to Fig. 1c, each individual and his/her k neighbours statically define a group (of size $k+1$). The fitness of individual i is associated with the accumulated payoff resulting from all PGGs in which he/she participates. Strategy evolution is implemented by using the finite population analogue of the replicator dynamics: at each time step each individual will adopt the strategy of a randomly chosen neighbour (if more fit) with a probability proportional to the fitness difference[16,29]. Consequently, the results become independent of the specific value used for the cost of cooperation c (we set c to 1). The results shown were obtained for communities of 10^3 individuals starting with 50% of cooperators randomly distributed on the population graph. The equilibrium fraction of cooperators results from averaging over 2,000 generations after a transient period of 10^5 generations. This procedure was repeated 100 times for 10 different realizations of each class of graph. Finally, the distributions depicted in Fig. 4 were obtained by averaging the fitness distributions over 50 scale-free graphs with average connectivity $z = 4$ and populations of 10^3 individuals, all cooperators.

Full Methods and any associated references are available in the online version of the paper at www.nature.com/nature.

Received 23 December 2007; accepted 20 March 2008.

1. Hardin, G. The tragedy of the commons. *Science* **162,** 1243–1248 (1968).
2. Binmore, K. G. *Game Theory and the Social Contract* Vol. 1, *Playing Fair* (MIT Press, Cambridge, MA, 1994).
3. Kollock, P. Social dilemmas: The anatomy of cooperation. *Annu. Rev. Sociol.* **24,** 183–214 (1998).
4. Hauert, C., De Monte, S., Hofbauer, J. & Sigmund, K. Volunteering as Red Queen mechanism for cooperation in public goods games. *Science* **296,** 1129–1132 (2002).
5. Milinski, M., Semmann, D., Krambeck, H. J. & Marotzke, J. Stabilizing the Earth's climate is not a losing game: Supporting evidence from public goods experiments. *Proc. Natl Acad. Sci. USA* **103,** 3994–3998 (2006).
6. Hofbauer, J. & Sigmund, K. *Evolutionary Games and Population Dynamics* (Cambridge Univ. Press, Cambridge, 1998).
7. Fehr, E. & Gachter, S. Altruistic punishment in humans. *Nature* **415,** 137–140 (2002).
8. Szabo, G. & Hauert, C. Phase transitions and volunteering in spatial public goods games. *Phys. Rev. Lett.* **89,** 118101 (2002).
9. Barabási, A. L. & Albert, R. Emergence of scaling in random networks. *Science* **286,** 509–512 (1999).
10. Ohtsuki, H. & Iwasa, Y. How should we define goodness?—reputation dynamics in indirect reciprocity. *J. Theor. Biol.* **231,** 107–120 (2004).
11. Nowak, M. A. & Sigmund, K. Evolution of indirect reciprocity. *Nature* **437,** 1291–1298 (2005).
12. Pacheco, J. M., Santos, F. C. & Chalub, F. A. Stern-judging: A simple, successful norm which promotes cooperation under indirect reciprocity. *PLoS Comput. Biol.* **2,** e178 (2006).
13. Hauert, C., Traulsen, A., Brandt, H., Nowak, M. A. & Sigmund, K. Via freedom to coercion: the emergence of costly punishment. *Science* **316,** 1905–1907 (2007).

14. Boyd, R. & Mathew, S. Behavior. A narrow road to cooperation. *Science* **316,** 1858–1859 (2007).
15. Szabo, G. & Hauert, C. Evolutionary prisoner's dilemma games with voluntary participation. *Phys. Rev. E* **66,** 062903 (2002).
16. Santos, F. C. & Pacheco, J. M. Scale-free networks provide a unifying framework for the emergence of cooperation. *Phys. Rev. Lett.* **95,** 098104 (2005).
17. Santos, F. C., Pacheco, J. M. & Lenaerts, T. Evolutionary dynamics of social dilemmas in structured heterogeneous populations. *Proc. Natl Acad. Sci. USA* **103,** 3490–3494 (2006).
18. Ohtsuki, H., Hauert, C., Lieberman, E. & Nowak, M. A. A simple rule for the evolution of cooperation on graphs and social networks. *Nature* **441,** 502–505 (2006).
19. Amaral, L. A., Scala, A., Barthelemy, M. & Stanley, H. E. Classes of small-world networks. *Proc. Natl Acad. Sci. USA* **97,** 11149–11152 (2000).
20. Albert, R. & Barabási, A. L. Statistical mechanics of complex networks. *Rev. Mod. Phys.* **74,** 47–97 (2002).
21. Dorogotsev, S. N. & Mendes, J. F. F. *Evolution of Networks: From Biological Nets to the Internet and WWW* (Oxford Univ. Press, Oxford, 2003).
22. Lieberman, E., Hauert, C. & Nowak, M. A. Evolutionary dynamics on graphs. *Nature* **433,** 312–316 (2005).
23. Nowak, M. A. & May, R. M. Evolutionary games and spatial chaos. *Nature* **359,** 826–829 (1992).
24. Nowak, M. A. Five rules for the evolution of cooperation. *Science* **314,** 1560–1563 (2006).
25. Boehm, C. *Hierarchy in the Forest: The Evolution of Egalitarian Behavior* (Harvard Univ. Press, Cambridge, MA, 1999).
26. Skyrms, B. *The Stag Hunt and the Evolution of Social Structure* (Cambridge Univ. Press, Cambridge, 2004).
27. Santos, F. C. & Pacheco, J. M. A new route to the evolution of cooperation. *J. Evol. Biol.* **19,** 726–733 (2006).
28. Traulsen, A., Nowak, M. A. & Pacheco, J. M. Stochastic dynamics of invasion and fixation. *Phys. Rev. E* **74,** 011909 (2006).
29. Hauert, C. & Doebeli, M. Spatial structure often inhibits the evolution of cooperation in the snowdrift game. *Nature* **428,** 643–646 (2004).

Supplementary Information is linked to the online version of the paper at www.nature.com/nature.

Acknowledgements F.C.S. acknowledges support from Fonds de la Recherche Scientifique, Belgium. M.D.S. and J.M.P. acknowledge financial support from Fundação para a Ciência e Tecnologia, Portugal.

Author Information Reprints and permissions information is available at www.nature.com/reprints. Correspondence and requests for materials should be addressed to J.M.P. (pacheco@cii.fc.ul.pt).

METHODS

Population structure. Population structure is represented by a graph; individuals occupy the vertices of the graph, and social interactions proceed along the edges. Figure 1 depicts the two topologies considered in this study. Figure 1a represents one-dimensional lattices, namely communities in which all individuals (nodes) are topologically equivalent, similar to those previously investigated. In Fig. 1b we provide a diagram of more realistic social structures, portraying populations in which different individuals have a distinct number of connections. Such strongly heterogeneous populations were obtained by means of the Barabási–Albert scale-free model based on growth and preferential attachment[9]. As is well known, realistic social structures fall somewhere between regular and scale-free graphs[19]. The blue circles in Fig. 2 were obtained on scale-free populations with 10^3 individuals generated in this way, with average connectivity $z = 4$. This implies that the smallest group in this population has three individuals[9]. In all simulations, the networks remain unchanged throughout evolution and each individual adopts a pure strategy: cooperator (C) or defector (D).

Public goods games. Every individual participates in all possible PGGs, accumulating the benefits and costs resulting from each of them. The accumulated value of the payoffs resulting from all possible PGGs contributes to individual fitness (neighbourhoods α, β, γ, δ and ε in Fig. 1c). In each PGG, the income of individual x will depend on the size of the group $k_x + 1$ (defined by the size of the neighbourhood centred on individual x; see Fig. 1), on the number n_C of Cs in his/her neighbourhood and on the multiplication factor r applied to the group investment. The incomes of a defector and a cooperator in one group are given by $P_D = crn_C/(k_x + 1)$ and $P_C = P_D - c$, respectively, in the case where all cooperators contribute the same cost c per game, such that the contribution of an individual is proportional to his/her number of social ties. In the opposite limit, we considered the case in which C individuals with k_x neighbours contribute a cost $c/(k_x + 1)$ per game, such that the individual contribution of each C equals c independently of the number of social ties. Hence, the payoff of an individual y with a strategy s_y (1 if C, 0 if D) associated with the PGGs centred in a individual x is given by

$$P_{y,x} = \frac{r}{k_x+1}\sum_{i=0}^{k_x}\frac{c}{k_i+1}s_i - \frac{c}{k_y+1}s_y$$

where $i = 0$ stands for x, s_i is the strategy of the neighbour i of x, and k_i is his/her degree.

Evolution. The network structure of the population defines not only the game interactions but also the structure through which strategy evolution proceeds. For non-repeated two-player games, this has been shown to constitute the most favourable model for cooperation[30]. After engaging in all games, the accumulated payoff is mapped onto individual fitness. After each game round, all strategies are updated synchronously by following the finite population analogue of the replicator dynamics[16,29]. When a site x with a payoff P_x is selected for update, a neighbour y (with a payoff P_y) is drawn at random between all k_x neighbours. If $P_x > P_y$, no update occurs. If $P_x < P_y$, x will adopt y's strategy with a probability given by $(P_y - P_x)/M$. M ensures the proper normalization and is given by the maximum possible difference between the payoffs of x and y. The results are robust with respect to changes both in the detailed form of the normalization factor or if we adopt an asynchronous update instead of the synchronous one.

Simulations. The results were obtained for communities with $N = 10^3$ individuals and an average connectivity of $z = 4$. Each equilibrium fraction of cooperators was obtained by averaging more than 2,000 generations after a transient period of 10^5 generations. We started with 50% of Cs randomly placed on the graph. Each data point depicted in Fig. 2 corresponds to an average over 1,000 simulations; that is, 100 runs for 10 different realizations of the same class of graph. Finally, the distributions depicted in Fig. 4 were obtained by averaging the fitness distributions over 50 scale-free graphs with $z = 4$ and populations of 10^3 individuals, all cooperators.

30. Ohtsuki, H., Nowak, M. A. & Pacheco, J. M. Breaking the symmetry between interaction and replacement in evolutionary dynamics on graphs. *Phys. Rev. Lett.* **98**, 108106 (2007).

doi: 10.1038/nature06940

Social diversity promotes the emergence of cooperation in public goods games

Francisco C. Santos[1], Marta D. Santos[2] & Jorge M. Pacheco[2]

[1] *IRIDIA*, Computer and Decision Engineering Department,

Université Libre de Bruxelles, Brussels, Belgium,

[2] *ATP*-group, CFTC, and Departamento de Fisica da Universidade de Lisboa,

Complexo Interdisciplinar, Av Prof. Gama Pinto 2, 1649-003 Lisboa, Portugal

SUPPLEMENTARY INFORMATION

15 pages and 8 figures.

Evolutionary dynamics of the Rich, the Poor, the Marginally and the Centrally connected

When population structure is associated with a heterogeneous social graph, one introduces diversity in the roles each individual plays in the community. In particular, when populations are structured following a scale-free distribution, the majority of individuals engage only in a few games, while a minority is able to participate in many games[27]. Depending on the size and number of the PGG each individual participates, the payoffs of an individual can rise to high values with respect to the population average, or may remain very low. In other words, the diversity introduced leads to another type of diversity which can be deduced from the fitness (or wealth, in a more economical sense) distribution. It is noteworthy, however, that the nature of the public good games makes the income of an individual depend not only on her number of social ties (her degree in the social graph), but also on the "degree" of her neighbors. In this sense, heterogeneous graphs lead to the appearance of several classes of individuals, both in what concerns the number of games in which they participate and also in what concerns their wealth.

Let us consider for simplicity, three classes of individuals regarding their number of social ties k_i on a scale-free network:

i) Low-Degree class, whenever $k_i < z$;

ii) Medium-Degree class, whenever $z \le k_i < \frac{k_{\max}}{3}$ and finally

iii) High-Degree class, whenever $\frac{k_{\max}}{3} \le k_i \le k_{\max}$,

encompassing the highly connected individuals (the hubs).

Let us also distinguish individuals in another group of three classes based on their personal wealth (fitness) Π_i:

i) Lower-Class, when $\Pi_i < \frac{\Pi_{total}}{3}$;

ii) Middle-Class, when $\frac{1}{3}\Pi_{total} \le \Pi_i < \frac{2}{3}\Pi_{total}$ *and*

iii) Upper-Class, when $\frac{2}{3}\Pi_{total} \le \Pi_i \le \Pi_{total}$,

where Π_{total} is the total wealth of the population at a given time of the evolutionary process.

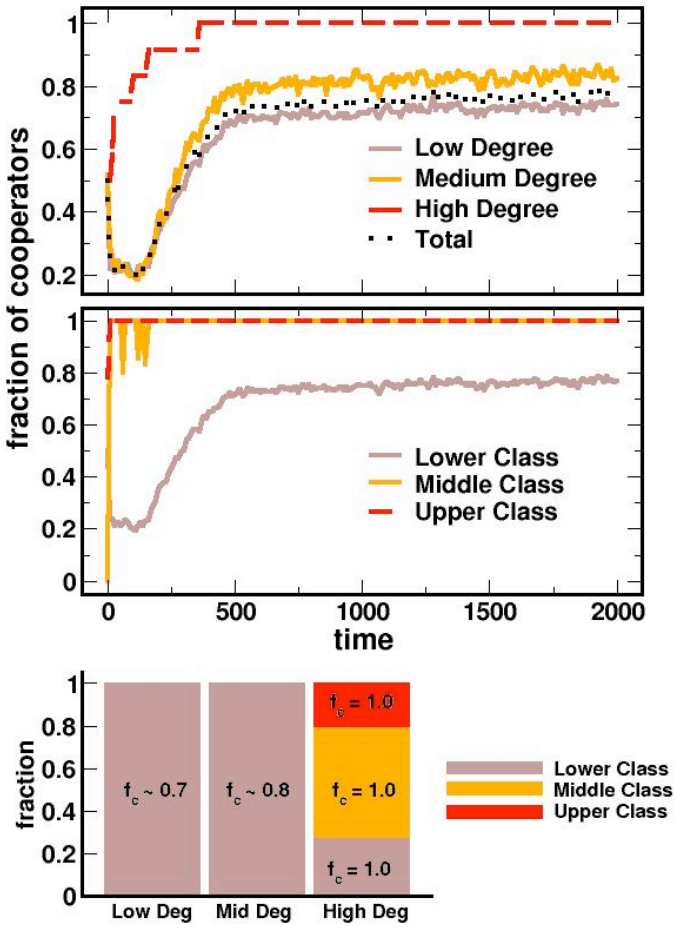

Figure S1. **Time-dependence of the fraction of cooperators on scale-free communities.**

In Figure S1 we plot the fraction of cooperators in the population for each of these 9 classes during evolution, when each individual invests the same amount irrespective of the number of PGG she participates. The time-dependent curves in Figure S1

provide a representative *run* for a multiplication factor $r=1.7$, that is, $\eta=0.34$ ($z=4$). For this value of η, cooperators dominate the population while unable to wipe out defectors.

In the upper panel, it is clear that individuals of High-Degree quickly become cooperators and remain so for the rest of the evolutionary process. On the contrary, Low-Degree and Medium-Degree classes start by adopting defector strategies. The more Low-Degree and Medium-Degree individuals adopt the **D** strategy, the more vulnerable they become to the influential role played by **C** hubs (High-Degree individuals). Consequently, the situation quickly reverts to a scenario in which **D**s survive only as individuals of Low-Degree and Medium-Degree.

The middle panel shows that high levels of wealth (fitness) – Upper-Class – are associated with **C**s. Moreover, no **D**s survive in the Middle-Class, being all relegated to the Lower-Class.

Finally, the lower panel summarizes together the information provided separately in the upper panels, correlating fitness, degree and strategy. Only individuals of High-Degree classes can achieve the Upper-Class in terms of wealth. On the other hand, the presence of **D**s in the population, both in the Lower-Degree and Medium-Degree classes, renders some High-Degree individuals unable to join the rest of the "hubs", remaining with a low wealth. The survival of **D**s is therefore detrimental to the overall wealth of the population and, individually, **D**s fare pretty badly in strongly heterogeneous communities, down to small values of the enhancement factor r. Diversity provides indeed a powerful mechanism to promote cooperation.

Dependence on population size and average connectivity

In the main text the discussion relied on simulations carried out for fixed population size N and fixed average degree z. Here we investigate how the results depend on these 2 quantities. To this end we carried out simulations for $N=500,1000$ and 5000 (for fixed $z=4$) and $z=4,16,32,64$ for fixed $N=500$. The results for fixed $z=4$ are shown in Figures S2 and S3, whereas results for fixed N and varying z are shown in Figure S4.

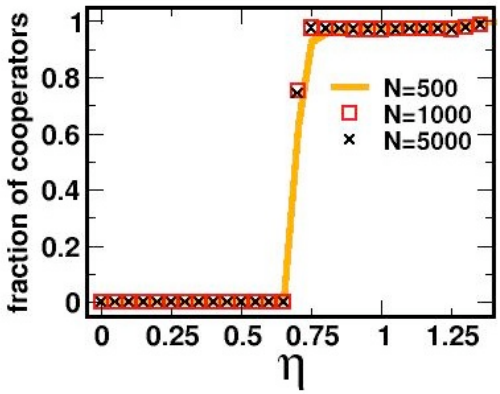

Figure S2. **Dependence of the evolution of cooperation on population size – regular graphs.** Results show that the evolution of cooperation is independent of population size for fixed average connectivity z. Populations are modeled in terms of regular graphs and each point corresponds to an average over 2000 runs for populations of sizes $N=500,1000,5000$. Note that, for regular graphs, the results do not depend on the cost paradigm: fixed cost per game, or fixed cost per individual.

Figures S2 and S3 evidence the negligible dependence of our results on the overall population size. We have checked that, for small z, the results are valid down to population sizes of $N\approx250$, below which the results are less smooth, given the increasing role of finite-size fluctuations on the evolutionary dynamics.

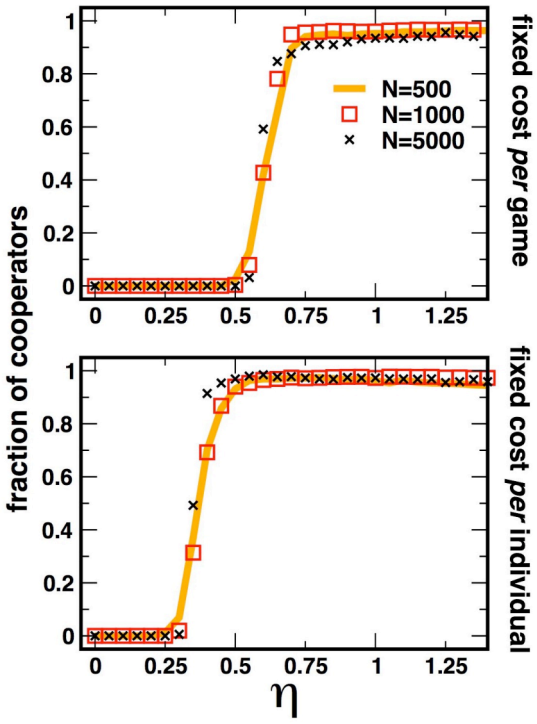

Figure S3. **Dependence of the evolution of cooperation on population size – Scale-free graphs.** Following the same notation of Figure S2, the results show that the evolution of cooperation is independent of population size for fixed average connectivity.

Concerning the dependence of the results on the average connectivity z (the number of links of the graph for fixed population size), several factors work against cooperative behavior when the average connectivity *z* increases.

First, the average size of the groups *(z+1)* increases. This factor induces an overall scaling of the value of the multiplication factor *r*: Since in Figure S4 we plot the fraction of cooperators as a function of η, this scaling is automatically included, which means that remaining differences between curves are due to other factors. The results of Figure S4 show that, irrespective of the cost paradigm, the critical value of η above which cooperators no longer get extinct does not qualitatively change with the average connectivity and is equivalent to an overall rescaling of *r*. This reflects the important role played by the average group size *(z+1)*.

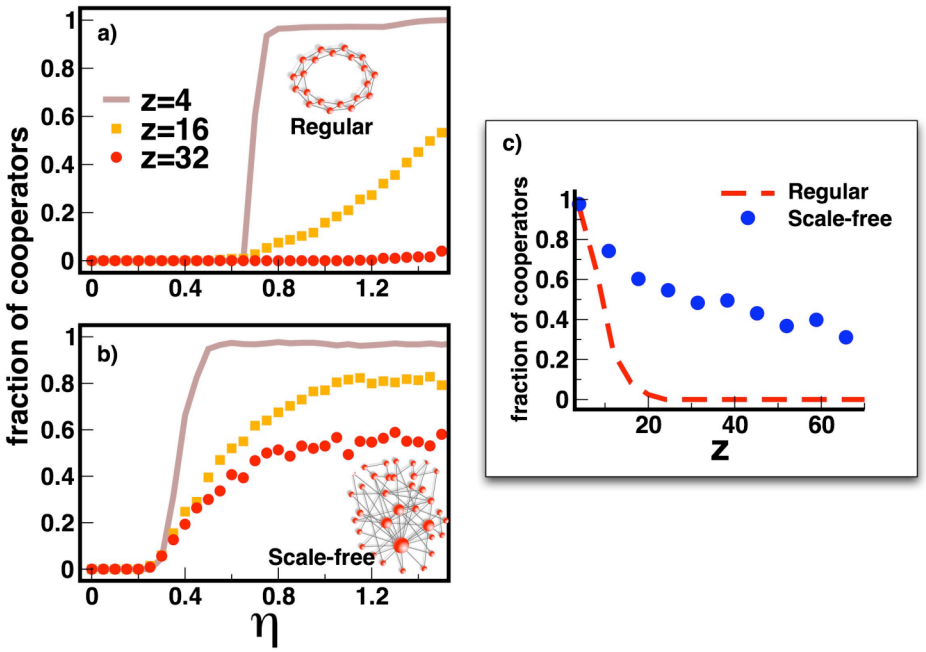

Figure S4. **Evolution of cooperation under PGG in populations with different average connectivity z.** Figures a) and b) follow the same notation and scheme of Figures 3 and 4. In c) we plot the final fraction of cooperators (for fixed η=0.8 in a region of coexistence of defectors and cooperators – see Figure S3). With increasing average degree z, results for PGG on graphs follow a trend similar to that obtained for simple two-player games on graphs[16] as one would expect (see main text for details). As z becomes sizeable cooperation will inevitably collapse as average group size increases and the overall degree of heterogeneity (on scale-free graphs) also decreases. Each value corresponds to an average over 100 runs for 20 network realizations and populations with N=500 individuals.

Furthermore, changing z towards a fully-connected graph corresponds to the limit case of having a PGG with the size of the whole (finite) population. In this limit, the presence of a single defector will always lead to the demise of cooperation, independently of the value of r. For instance, Figure S4 shows that, on regular networks, $z = 16$ is enough to reduce significantly the final number of cooperators, even when η>1. Similar to simple 2-player games, spatially constrained populations are only able to sustain sizeable levels of cooperative behavior on sparse graphs[8, 18, 23]

– lack of diversity leaves survival of cooperation contingent on the feasibility of cooperators to form tight communities. With increasing connectivity, these tight communities become increasingly vulnerable to exploitation, favouring defectors.

Figure S4-c also shows that the significant boost of cooperation obtained for scale-free graphs compared to regular graphs is a robust feature, being a slowly decreasing function of the average connectivity z. The results of Figure S4 correspond to the situation of a fixed investment per individual, but the conclusions remain qualitatively independent of the investment scheme adopted.

Cooperators and Defectors on the star(s)

In the scale-free graphs we have used to model heterogeneous populations, individuals have never less than 2 neighbors. In Fig. S5-a we provide a detail of such a graph. This feature determines the occurrence of short closed loops (for example triangles, which are responsible for the small, yet non-zero value of the cluster coefficient exhibited by these graphs) that precludes simple analytic treatments.

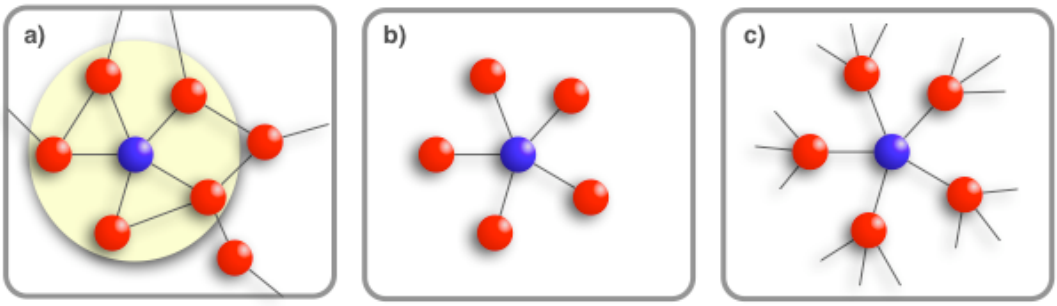

Figure S5. **The star and generalized star graphs.** We shall employ the simple star graph depicted in b), in this case 1 center and 5 leaves, as the simplest abstraction of the sub-graph selected in panel a). In panel c) we generalize the star such that every leaf has $k-1$ links, the overall structure exhibiting no loops.

In order to demonstrate the mechanism responsible for the emergence of cooperation in Figure 2-b, we resort here to the simplest possible (and most disadvantageous) situation for a cooperator – that of a single **C** in a population of **D**s only. Moreover, we shall start by "abstracting" from the connections of the neighbors of this **C** to other **D**s, which naturally leads to a star-graph, Figure S5-b. To the extent that the single **C** may have a larger fitness than any of her **D**-neighbors, the **C**-strategy will spread. The fact that on a star there are only 2 types of nodes - center and leaves - and no loops clearly simplifies the mathematical analysis.

Let us then consider a star of size N : 1 center (h) and N-1 leaves (l) - with the single **C** located on the center (Figure S5-b). In such scenario (if the **C** is placed on a leaf her fitness will never exceed that of a **D** in the center), the fitness (Π) of the **C** is given by

$$\Pi(h) = \frac{rc}{N^2} + (N-1)\frac{r}{2}\frac{c}{N} - c$$

whereas the fitness of any of the **D**s (leaves) reads

$$\Pi(l) = \frac{rc}{N^2} + \frac{rc}{2N} .$$

From the expressions above, the **C**-strategy will spread whenever

$$\Pi(h) - \Pi(l) > 0 \Leftrightarrow r > \frac{2}{1-2/N}$$

a *decreasing* function of N. In other words, not only is it possible for a single **C** to become advantageous, but also the critical value of the multiplication factor r decreases with increasing number of leaves. This result suggests that the feasibility of the **C**–strategy to spread increases with the connectivity of the node on which the **C** is located.

Clearly, the star is a gross simplification of a realistic population structure; a useful, yet simple, structure, is the generalized star depicted in Figure S5-c, in which every leaf has *k-1* external links to other **D**-neighbors. In this case we obtain

$$r > \frac{k}{1-2/N}$$

which remains a decreasing function of N (for fixed k). Clearly, invasion is easier the larger the difference (diversity) between the connectivities of the center and of the leaves. On the other hand, whenever $k=N$, we obtain the limit of a "homogeneous generalized star", in which we may write for the critical threshold

$$r > \frac{N}{1-2/N}.$$

On scale-free populations, the majority of individuals have few connections, whereas a few highly connected individuals ensure the overall connectivity of the entire population. Naturally, most of the highly connected individuals (hubs) connect to individuals of low connectivity, which provide excellent conditions for a **C** located on a hub to spread to other nodes.

So far we have seen that **C**s can spread more efficiently from centers to leaves on heterogeneous graphs. But how do **C**s invade a **D** hub ? Similar to the star-model considered above, the double star model below provides a simple illustration of the evolutionary dynamics of "hub-invasion".

Let us consider the generalized double-star configuration depicted in Figure S6.

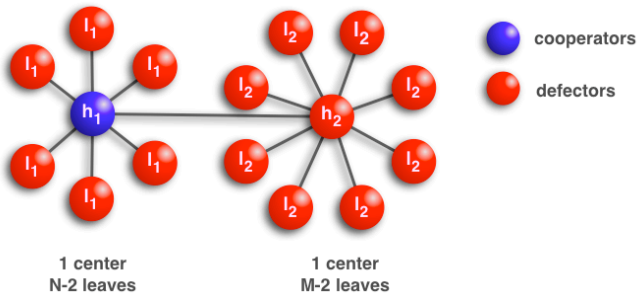

Figure S6. **The double-star graph.** In the double star depicted, we have 2 centers (h_1 and h_2) the left one with *N-2* leaves and the right one with *M-2* leaves. This simple (heterogeneous) structure allows us to inspect the conditions under which a single cooperator in h_1 may take over a defector in h_2. We shall in fact consider a generalized double-star, in which case each l_1 has *k-2* external links (no loops) whereas each l_2 has *j-2* external links.

We have 2 centers (hubs h_1 and h_2) with *N-2* and *M-2* leaves respectively, and 1 link connecting the two centers. Each of the *N-2* leaves has additional *k-2* external links, whereas each of the *M-2* leaves has *j-2* external links. Let us place a **C** on h_1 with the rest of the nodes as **D**s. In this case, the **C**-strategy will spread to h_2 whenever

$$\Pi(h_1) - \Pi(h_2) > 0 \Leftrightarrow r > \frac{kN}{N-2} \equiv \alpha \,,$$

whereas the **C**-strategy will spread to the leaves of h_1 whenever

$$\Pi(h_1) - \Pi(l_1) > 0 \Leftrightarrow r > \frac{kMN}{k + M(N-3)} \equiv \beta \ .$$

Since $\alpha < \beta$ (whenever $M > k$), it will be easier for the **C** sitting on h_1 to invade h_2 than the leaves of h_1. In fact, invasion of h_2 depends only on the number of leaves of h_1 and of their connectivity: the larger the leaf-connectivity the harder it will be to invade h_2, whereas the larger the connectivity of h_1, the easier it will be to invade h_2. In particular, notice that the invasion condition does not depend on the connectivity of h_2 ! In other words, even on "generalized" double-stars, **C**s will manage to expand to the extent that $r > \beta$.

In the remainder of this section, we would like to use the simple double-star to show how **C**s resist invasion by **D**s. This mechanism is crucial to the survival of cooperation[27]. To this end we introduce a **D** in h_1 in a population of all **C**s, as shown in Figure S7-a.

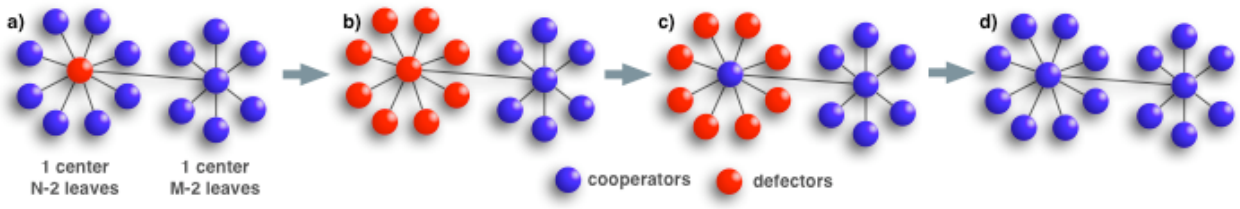

Figure S7. **The demise of a successful D.** Panel a) shows a single **D** in a sea of **C**s. Whenever the **D**-fitness is larger than the fitness of any of the **C**s, the **D**-strategy will spread. We show that such spreading occurs preferentially to the leaves, which contributes to reduce the fitness of the center **D**, making it vulnerable to a take over by the central **C**. Such negative feedback mechanism of the **D**s leads to their own demise.

Whether the single **D** is the fittest individual in the double star will depend on the balance between N and M. Indeed, we obtain

$$\Pi(h_2) > \Pi(h_1) \Leftrightarrow r > \frac{4M}{M^2 - 4 - M(N-2)}$$

and to the extent that r satisfies the inequality above, the **C**-center will have a larger fitness than the **D**-center and consequently will spread the **C**-strategy onto the **D**-star. Another interesting condition is the one equating the fitness of both centers if, instead of a neighborhood with **C**s only, the **D**-center has only $k \leq N-2$ **C** neighbors. We may write

$$\Pi(h_2) > \Pi(h_1^{\,k}) \Leftrightarrow r > \frac{4M}{M^2 - 4 - Mk}.$$

Let us imagine, however, that we start with *k=N-2* and (for example) r is such that $\Pi(h_2) < \Pi(h_1)$. In this case the **D** strategy will spread. However, unlike the symmetric situation discussed before, here we get

$$\left[\Pi(h_1) - \Pi(l_1)\right] - \left[\Pi(h_1) - \Pi(h_2)\right] = \frac{rc}{4M^2}\left[4 + M\left(M^2 + M - 8\right)\right] > 0 \ (M > 2)$$

Consequently, it is more likely that **D** will spread to l_1 than to h_2, given that each player will imitate her neighbor with a probability proportional to the payoff difference. This means the neighborhood of h_1 will turn into **D** before h_2, creating the pattern of Figure S7-b (in practice, it need not reach the configuration in Figure S7-b as whenever $\Pi(h_2) > \Pi(h_1^k)$ the **C**-center may actually invade the **D**-center). In other words, **D**s are victims of their own success, as they efficiently spread their strategy to the "weak" neighbors, reducing their own fitness and becoming prone to be taken over by the **C**-center.

At this stage (Figure S7-b), the payoffs of both centers are

$$\Pi(h_1) = \frac{rc}{MN} + \frac{r}{M}\left(\frac{(M-2)c}{2} + \frac{c}{M}\right)$$

$$\Pi(h_2) = \Pi(h_1) + rc\frac{M^2 - 4}{4M} - c$$

such that h_2 easily becomes advantageous with respect to h_1 (M>2)

$$\Pi(h_2) > \Pi(h_1) \Leftrightarrow r > \frac{4M}{M^2 - 4}.$$

In other words, evolutionary dynamics leads the population into the configuration of Figure S7-c (or, even better, the **D**-center will be taken over by the **C**-center before all **C**s on the leaves of the left turn into **D**s). At this stage we return to a configuration similar to the one of Figure S6, but more beneficial for **C**s: The spreading of the **C**-strategy to the leaves on the left will take place whenever ($\{M, N\} > 2$)

$$r > \frac{2M^2N}{2(M+N)+2MN(M-1)-3M^2}$$

which clearly favors invasion of the leaves, even for small N and M. In practice, simulation results show (Figure S8) that **C**s will tend to dominate the population.

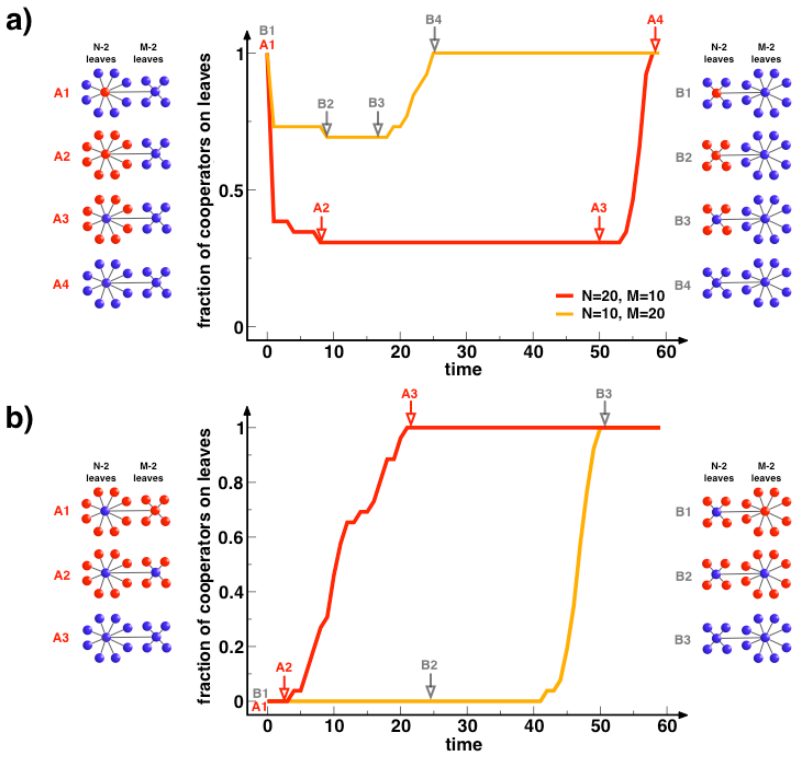

Figure S8. **Evolution of cooperation under PGG on double stars.** Figures a) and b) provide a typical scenario for time evolution of the fraction of **C**s on the leaves of double-star graphs. **a)** We start with a single **D** both in the largest center (red line) and in the smallest center (orange line) (configurations A1 and B1). The overall behavior shows that the **D** invades the leaves of her star (A2 and B2), after which is invaded by the **C** in the center of the second star (A3 and B3). Subsequently, the remaining defectors on the leaves are invaded by **C**s (B4) (see Figure S7). As expected, the relative connectivity of both centers (**C** and **D**) determines the overall time required for invasion (red line: r=1.3, N=20 and M=10 ; orange line: r=1.3, N=10 and M=20). **b)**, We start with a single **C** located in one of the centers in a population of **D**s (A1 and B1), with r=2.8 (r>β>α, see main text). The **C**-center starts by invading the **D**-center (A2 and B2), after which the C-strategy spreads to all leaves (A3 and B3). Given that the ability of the **C**-center to invade the **D**-center increases with the **C**-center connectivity, $N>M$ leads to a faster invasion than $N<M$.

Finally, it is worth noting that the introduction of small loops in the double star above leads to important changes in the overall evolutionary dynamics; not only the time for **C**-dominance decreases, but also the critical values of r above which **C**s dominate also decreases, a feature which is difficult to capture analytically.